

Tomlinson-Harashima Precoding-Aided Multi-Antenna Non-Orthogonal Multiple Access

Jungho So, *Student Member, IEEE*, Youngchul Sung[†], *Senior Member, IEEE*,
and Yong H. Lee, *Senior Member, IEEE*

Abstract—In this paper, Tomlinson-Harashima Precoding (THP) is considered for multi-user multiple-input single-output (MU-MISO) non-orthogonal multiple access (NOMA) downlink. Under the hierarchical structure in which multiple clusters each with two users are formed and served in the spatial domain and users in each cluster are served in the power domain, THP is applied to eliminate the inter-cluster interference (ICI) to the strong users and enlarge the dimension of the beam design space for mitigation of ICI to weak users as compared to conventional zero-forcing (ZF) inter-cluster beamforming. With the enlarged beam design space, two beam design algorithms for THP-aided MISO-NOMA are proposed. The first is a greedy sequential beam design with user scheduling, and the second is the joint beam redesign and power allocation. The two design problems lead to non-convex optimization problems. An efficient algorithm is proposed to solve the non-convex optimization problems based on successive convex approximation (SCA). Numerical results show that the proposed user scheduling and two beam design methods based on THP yield noticeable gain over existing methods.

Index Terms—Non-orthogonal multiple access, Tomlinson-Harashima precoding, multi-user MISO, successive convex approximation

I. INTRODUCTION

Power-domain NOMA also known as multi-user superposition transmission (MUST) is one of the promising technologies for 5G wireless communication to enhance the spectral efficiency [1], [2]. Conventionally, the wireless communication resources such as time, bandwidth and spatial domains were divided into multiple orthogonal resource blocks, and one user is assigned to each orthogonal resource block. Unlike such conventional orthogonal multiple access, in NOMA the base station (BS) serves multiple users in a single orthogonal resource block based on superposition coding and successive interference cancellation (SIC) by exploiting the power domain. Initially, NOMA was studied for single-input single-output (SISO) systems [3]–[6], but recently there have been extensive research works to extend NOMA to multiple-antenna systems [7]–[13]. NOMA in multiple-antenna systems is attractive since it increases the spectral efficiency further on top of the multiple antenna technology. On the contrary to single-antenna

NOMA in which only the power domain exists, in multiple-antenna NOMA there exist spatial and power domains to be exploited for user multiplexing and data transmission. These joint spatial and power domains should be used efficiently for operation of multiple-antenna NOMA, and corresponding user scheduling/grouping, beam design and power allocation are of great importance for good performance of multiple-antenna NOMA.

A. Related Works and Motivation

In this paper, we consider the MU-MISO NOMA downlink. Although there exists vast literature for MU-MISO NOMA, we discuss only the most related works to our work in this subsection. Even though the problem of supporting multiple users in MU-MISO NOMA downlink can be approached by multi-user SIC without hierarchy as in [10], we here consider the hierarchical approach as in [7], [9], [11]–[13], which is simple and attractive from the perspective of design and SIC complexity. In the hierarchical approach, simultaneously-served users are first grouped into multiple clusters, and then multiple clusters are supported in the spatial domain while users in each cluster are supported in the power domain. That is, users in each cluster share the same spatial beam vector and are supported by superposition coding and SIC. In these works as well as in many other MU-MISO NOMA works, researchers assume that two users (one strong user and one weak user) are grouped in each cluster, considering signaling overhead and SIC error propagation [7], [9], [12]–[15]. We make this assumption too in this paper. Then, the main problem in the hierarchical approach to MU-MISO NOMA is the joint design of beams, power allocation and user scheduling. However, this joint design of beams, power allocation and user scheduling is a complicated problem. Hence, under the assumption of two-user grouping for each cluster, to make the joint design problem tractable, the step of beam design for MU-MISO NOMA was simplified by designing the beams as linear ZF beams based on strong users' channels, and then two users in each cluster share the same beam [9], [12]. The reason for this beam design strategy is to keep up to the asymmetric NOMA principle that the strong users having high-quality channels are not limited by noise or interference, whereas the weak users having bad channels are limited by noise. Under this hierarchical MU-MISO NOMA structure with the beams designed as ZF beams for strong users, several user scheduling/grouping and/or power allocation methods were proposed [7], [9], [12], [13]. Although this linear ZF beam design

[†]Corresponding author

The authors are with School of Electrical Engineering, KAIST, Daejeon 305-701, South Korea. E-mail: jhso@kaist.ac.kr; ysung@ee.kaist.ac.kr; yohlee@kaist.ac.kr. This work was supported in part by 'The Cross-Ministry Giga KOREA Project' grant funded by the Korea government (MSIT) (No.GK17N0100, 5G Mobile Communication System Development based on mmWave) and in part by 'The Cross-Ministry Giga KOREA Project' grant funded by the Korea government (MSIT) (No.GK17S0400, Research and Development of Open 5G Reference Model).

strategy simplifies the overall problem for the hierarchy-based MU-MISO NOMA, it has limitation. Suppose that we have N_t transmit antennas and N_t clusters each consisting of one strong user and one weak user. In case that the beams are designed as the ZF beams based on the strong users' channels, the beam for each cluster should be in the one-dimensional orthogonal space of the linear space spanned by the remaining $N_t - 1$ clusters' strong users' channels. Hence, there is no freedom in the beam design and ICI is controlled solely by weak user selection. Thus, by enlarging the dimension of the beam design space, we can improve the weak user performance in addition to weak user selection.

B. Contributions of the Paper

In this paper, we consider the aforementioned hierarchical design for MU-MISO NOMA downlink, and propose two beam design methods together with corresponding user scheduling, by applying the transmitter-side non-linear processing technique, THP. The contributions of this paper are summarized below:

- In Section II, we provide a framework for application of THP to single-cell MU-MISO NOMA downlink systems. We show that by applying THP to completely remove ICI to the strong users, the dimension of the beam design space for the k -th cluster is increased to $N_t + 1 - k$ which is larger than that of simple ZF beam design $N_t + 1 - N_c$, where N_t is the number of transmit antennas at the BS and N_c is the number of clusters. The increased design freedom can be exploited to mitigate ICI to the weak users.

- In Section III-A, we propose a user scheduling algorithm together with a greedy sequential beam design method by considering the rates of THP-aided MU-MISO NOMA. The proposed user scheduling algorithm first selects the strong users based on the semi-orthogonal user selection (SUS) algorithm [16] and then selects the weak users sequentially with the beams designed in a sequential greedy manner.

- In Section III-B, we solve the joint problem of beam redesign and power allocation after user selection to further improve the performance over the sequential greedy beam design method. This joint optimization problem reduces to a non-convex problem. We propose an efficient algorithm to solve this joint optimization problem based on SCA and prove that the algorithm converges to a stationary point of the joint optimization problem.

Numerical results show that the proposed methods in this paper yield noticeable gain as compared to the existing methods for MU-MISO NOMA downlink.

C. Notation and Organization

We will use standard notations in this paper. Vectors and matrices are written in boldface with matrices in capitals. All vectors are column vectors. For a matrix \mathbf{A} , \mathbf{A}^T , \mathbf{A}^H , \mathbf{A}^{-1} , and $\text{Tr}(\mathbf{A})$ indicate the transpose, conjugate transpose, inverse, and trace of \mathbf{A} , respectively. $\mathcal{C}(\mathbf{A})$ and $\mathcal{C}^\perp(\mathbf{A})$ denote the linear subspace spanned by the columns of \mathbf{A} and its orthogonal complement, respectively. $\Pi_{\mathbf{A}}$ and $\Pi_{\mathbf{A}}^\perp$ are the projection matrices to $\mathcal{C}(\mathbf{A})$ and $\mathcal{C}^\perp(\mathbf{A})$, respectively.

$[\mathbf{a}_1, \dots, \mathbf{a}_n]$ denotes the matrix composed of column vectors $\mathbf{a}_1, \dots, \mathbf{a}_n$. $\|\mathbf{a}\|$ represents the 2-norm of vector \mathbf{a} . \mathbf{I}_n and \mathbf{O} denote the $n \times n$ identity matrix (the subscript is omitted when unnecessary) and all-zero matrix with proper size, respectively. For a random vector \mathbf{x} , $\mathbb{E}\{\mathbf{x}\}$ denotes the expectation of \mathbf{x} , and $\mathbf{x} \sim \mathcal{CN}(\boldsymbol{\mu}, \boldsymbol{\Sigma})$ means that \mathbf{x} is circularly-symmetric complex Gaussian-distributed with mean vector $\boldsymbol{\mu}$ and covariance matrix $\boldsymbol{\Sigma}$. $\iota := \sqrt{-1}$.

The remainder of this paper is organized as follows. In Section II, the system model and preliminaries are described. In Section III, the proposed method for user scheduling, beam design and power allocation for THP-aided MU-MISO NOMA systems is presented. Numerical results are provided in Section IV, followed by conclusions in Section V.

II. SYSTEM MODEL

In this paper, we consider a single-cell MU-MISO NOMA downlink system consisting of a BS with N_t transmit antennas and K_{tot} single-antenna users. We assume the following for our system model:

A.1 (User Partition): We assume that the total K_{tot} users in the system are partitioned into two user sets, \mathcal{K}_1 and \mathcal{K}_2 , according to their channel strength, as in [13], [17]. \mathcal{K}_1 is the set of users with strong channels and \mathcal{K}_2 is the set of users with weak channels. The cardinality of each set is given by $|\mathcal{K}_1| = |\mathcal{K}_2| = K_{tot}/2$.

A.2 (User Scheduling and Clustering): Taking signalling overhead and SIC error propagation into account, we assume that two users are grouped in each cluster as in [7], [9], [12], [15]. We assume that N_c ($\leq N_t$) clusters are constructed in total and each cluster is composed of one strong-channel user (simply strong user) from \mathcal{K}_1 and one weak-channel user (simply weak user) from \mathcal{K}_2 . In each cluster, the strong user performs SIC before decoding its own message, and the weak user decodes its own data by treating the interference from the strong user as noise. For each cluster, we will refer to the strong user as User 1 and the weak user as User 2. The details of user scheduling and grouping will be presented in Section III.

A.3 (Spatial Multiplexing): To implement spatial multiplexing on top of two-user superposition coding in MU-MISO NOMA, we assume that two users in each cluster are multiplexed in the power domain with superposition coding and SIC as mentioned in Assumption A.2, while multiple clusters are multiplexed in the spatial domain by inter-cluster beamforming. To do so, we assume that a beam vector is assigned to each cluster and the strong and weak users in each cluster share the beam vector assigned to the cluster. Under this assumption, the transmit signal \mathbf{x} of the BS for one scheduling interval is given by

$$\mathbf{x} = \sum_{k=1}^{N_c} \mathbf{w}_k \tilde{x}_k(\{d_{k1}, d_{k2}, p_{k1}, p_{k2}\}_{k=1}^{N_c}), \quad (1)$$

where \mathbf{w}_k is the $N_t \times 1$ beam vector assigned to Cluster k such that $\|\mathbf{w}_k\|^2 = 1$, and $\tilde{x}_k(\{d_{k1}, d_{k2}, p_{k1}, p_{k2}\}_{k=1}^{N_c})$ is the scalar signal of Cluster k generated from the data symbols and the power values $\{d_{k1}, d_{k2}, p_{k1}, p_{k2}, k = 1, \dots, N_c\}$. Here, d_{k1}

and d_{k2} are the data symbols of Users 1 and 2, respectively, and p_{k1} and p_{k2} are the transmit power values assigned to Users 1 and 2, respectively, such that

$$p_{k1} + p_{k2} \leq p_k, \quad \sum_{k=1}^{N_c} p_k \leq P, \quad (2)$$

where p_k is the transmit power assigned to Cluster k and P is the total transmit power.

A.4 (Symbol Modulation): We assume that the user data symbols d_{k1} and d_{k2} are generated from M -ary quadrature-based modulation such as M -ary amplitude modulation (M -QAM) or M -ary phase shift keying (M -PSK), and assume that $\mathbb{E}\{|d_{k1}|^2\} = \mathbb{E}\{|d_{k2}|^2\} = 1$.

Under the above assumptions, the received signals of Users 1 and 2 in Cluster k are given by

$$y_{k1} = \mathbf{h}_{k1}^H \mathbf{w}_k \tilde{x}_k + \sum_{j \neq k} \mathbf{h}_{k1}^H \mathbf{w}_j \tilde{x}_j + n_{k1}, \quad (3)$$

$$y_{k2} = \mathbf{h}_{k2}^H \mathbf{w}_k \tilde{x}_k + \sum_{j \neq k} \mathbf{h}_{k2}^H \mathbf{w}_j \tilde{x}_j + n_{k2} \quad (4)$$

where y_{k1} and y_{k2} are the received signals of Users 1 and 2 in Cluster k , \mathbf{h}_{k1} and \mathbf{h}_{k2} are the $N_t \times 1$ channel vectors from the BS to Users 1 and 2 in Cluster k , and n_{k1} and n_{k2} are the additive white Gaussian noise (AWGN) at Users 1 and 2 in Cluster k from distribution $\mathcal{CN}(0, \sigma^2)$, respectively. Here, the dependence of the cluster scalar signal \tilde{x}_k on $\{d_{k1}, d_{k2}, p_{k1}, p_{k2}\}$ is not shown for notational simplicity. Note that the last two terms in each of the right-hand sides (RHSs) of (3) and (4) are ICI and AWGN.

A widely-considered way to combine MU-MISO with NOMA is to use ZF inter-cluster beamforming for design of $\mathbf{w}_1, \dots, \mathbf{w}_{N_c}$ and to design the cluster scalar signal \tilde{x}_k as [9], [12]–[14]

$$\tilde{x}_k(\{p_{k1}, p_{k2}, d_{k1}, d_{k2}\}_{k=1}^{N_c}) = \sqrt{p_{k1}} d_{k1} + \sqrt{p_{k2}} d_{k2}. \quad (5)$$

ZF beamforming is simple and effective to eliminate other user interference. However, when it is applied to remove the ICI in MU-MISO NOMA, it cannot remove the ICI for all users due to lack of spatial dimensions. That is, in the case of $N_c = N_t$ with two-user grouping, we have $2N_t$ users but only N_t transmit antennas. Hence, many researchers proposed using ZF beamforming to eliminate the ICI at the strong users [9], [12]–[14]. This is because in NOMA, two users in each cluster are chosen so that the strong user has a high signal-to-noise ratio (SNR) channel, whereas the weak user is noise-limited. The high SNR channel is maintained by SIC for the strong user. On the other hand, interference is allowed to the weak user with high noise anyway but high power is assigned to the weak user to boost its signal-to-interference-plus-noise ratio (SINR). Hence, to be consistent with this design principle of NOMA, ZF beamforming is applied to eliminate ICI at the strong users. In this case, the beam vector for Cluster k is given by a unit-norm vector as

$$\mathbf{w}_k \in \mathcal{C}^\perp(\mathbf{H}_1^{-k}), \quad (6)$$

where

$$\mathbf{H}_1^{-k} := [\mathbf{h}_{11}, \dots, \mathbf{h}_{k-1,1}, \mathbf{h}_{k+1,1}, \dots, \mathbf{h}_{N_c,1}]. \quad (7)$$

With the ZF beamforming vectors $\mathbf{w}_1, \dots, \mathbf{w}_{N_c}$, we have $\mathbf{h}_{k1}^H \mathbf{w}_j = 0, \forall j \neq k$, and the ICI term in the received signal (3) of the strong user disappears.

However, the limitation of this ZF inter-cluster beamforming for MU-MISO NOMA is that it eliminates the design freedom for the beam vectors $\mathbf{w}_1, \dots, \mathbf{w}_{N_c}$. In the case of $N_t = N_c$, the orthogonal space of the linear space spanned by the columns of the matrix \mathbf{H}_1^{-k} in (7) has only one dimension almost surely for independently realized channel vectors $\mathbf{h}_{11}, \dots, \mathbf{h}_{N_c,1}$, and thus the beam vector \mathbf{w}_k for Cluster k is predetermined by the channel vectors. Hence, we do not have control over \mathbf{w}_k and the ICI at the weak user in (4) is controlled only by user selection. However, user selection alone has limitation in handling the ICI to the weak user.

To overcome this limitation of the ZF inter-cluster beamforming*, in this paper we adopt THP at the BS to provide extra freedom to the design of the inter-cluster beamforming vectors $\mathbf{w}_1, \dots, \mathbf{w}_{N_c}$. The application of THP is possible in a MU-MISO NOMA BS since the BS knows all data symbols for all downlink users. In the below, we briefly summarize the basic idea of THP and explain how THP can be applied to the MU-MISO NOMA downlink. Based on this, we will proceed to user scheduling and beam design in Section III.

A. Preliminary: Tomlinson-Harashima Precoding

THP is a nonlinear precoding technique which eliminates other user interference from the transmitter side based on channel state information at the transmitter (CSIT) like dirty paper coding (DPC), but it is a practical and usable technique [18]–[20]. To explain THP in MU-MISO downlink, let us consider a single-cell MU-MISO system with a BS with N_t transmit antennas and $N_c (\leq N_t)$ single-antenna users. The $N_c \times 1$ received signal vector \mathbf{y} composed of the received signals y_1, \dots, y_{N_c} of the N_c users is given by

$$\mathbf{y} = \mathbf{H}^H \mathbf{s} + \mathbf{n} \quad (8)$$

where $\mathbf{y} = [y_1, y_2, \dots, y_{N_c}]^T$ is the $N_c \times 1$ received signal vector with y_k being the received signal of the k -th user; $\mathbf{H} = [\mathbf{h}_1, \mathbf{h}_2, \dots, \mathbf{h}_{N_c}]$ is the $N_t \times N_c$ channel matrix with \mathbf{h}_k being the $N_t \times 1$ MISO channel vector from the BS to the k -th user; \mathbf{s} is the $N_t \times 1$ transmit signal vector; and $\mathbf{n} = [n_1, n_2, \dots, n_{N_c}]^T$ is the $N_c \times 1$ noise vector with $n_k \stackrel{i.i.d.}{\sim} \mathcal{CN}(0, \sigma^2)$. Note that the $N_t \times N_c$ matrix \mathbf{H} is a square or tall matrix since $N_t \geq N_c$. By applying QR decomposition to \mathbf{H} , we have

$$\mathbf{H} = \mathbf{Q}\mathbf{R}, \quad \mathbf{H}^H = \mathbf{R}^H \mathbf{Q}^H = \mathbf{L}\mathbf{Q}^H, \quad (9)$$

where $\mathbf{L} (= \mathbf{R}^H)$ is an $N_c \times N_c$ lower-triangular matrix and \mathbf{Q} is an $N_t \times N_c$ matrix whose column vectors $\{\mathbf{q}_k, k = 1, \dots, N_c\}$ are orthogonal to each other with $\|\mathbf{q}_k\|^2 = 1$ for $k = 1, \dots, N_c$. Let $\mathbf{s} = \mathbf{Q}\tilde{\mathbf{s}}$, where $\tilde{\mathbf{s}} = [\tilde{s}_1, \dots, \tilde{s}_{N_c}]^T$ is an

*One can consider minimum mean-square error (MMSE) inter-cluster beamforming to yield better performance at low SNR. However, MMSE beamforming converges to ZF beamforming at high SNR and the issue of the beam space restriction does not change with MMSE inter-cluster beamforming. That is, when the channel vectors $\mathbf{h}_{11}, \dots, \mathbf{h}_{N_c,1}$ are given, the MMSE beam vectors are determined.

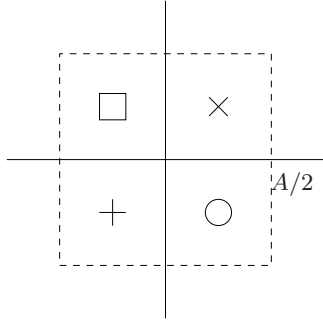


Fig. 1: 4-QAM constellation points

$N_c \times 1$ effective transmit signal vector and \tilde{s}_k is the transmit signal for the k -th user. (Note that in this case \mathbf{Q} is the transmit beamforming matrix and \mathbf{q}_k is the beam vector for the k -th user carrying \tilde{s}_k .) Then, the received signal vector \mathbf{y} can be rewritten as

$$\mathbf{y} = \mathbf{H}^H \mathbf{s} + \mathbf{n} = \mathbf{L}\mathbf{Q}^H \mathbf{Q} \tilde{\mathbf{s}} + \mathbf{n} = \mathbf{L} \tilde{\mathbf{s}} + \mathbf{n} \quad (10)$$

and the corresponding received signal at the k -th user is given by

$$y_k = l_{kk} \tilde{s}_k + \sum_{j=1}^{k-1} l_{kj} \tilde{s}_j + n_k, \quad k = 1, \dots, N_c, \quad (11)$$

where l_{kj} is the element of \mathbf{L} at the k -th row and j -th column, the first term in the RHS of (11) is the desired signal of the k -th user, and the second term in the RHS of (11) is the interference from the first to $(k-1)$ -th users to the k -th user.

THP exploits the fact that in digital communication the symbols for each user are modulated symbols existing only on a certain modulation constellation. Suppose that the actual data symbol d_k carried in the transmit signal \tilde{s}_k is from the set of M -ary quadrature-based modulation constellation points. For the purpose of explanation, consider the constellation $\{(+\frac{A}{4}, +\frac{A}{4}), (+\frac{A}{4}, -\frac{A}{4}), (-\frac{A}{4}, +\frac{A}{4}), (-\frac{A}{4}, -\frac{A}{4})\}$ of 4-QAM here, as shown in Fig. 1. In order to eliminate interference $\sum_{j=1}^{k-1} l_{kj} \tilde{s}_j$ in the received signal of the k -th user (11), THP subtracts the interference and uses modulo operation in a sequential manner at the transmitter side as follows: [20]

$$\tilde{s}_1 = d_1 \quad (12)$$

$$\tilde{s}_2 = \text{mods}_A \left(d_2 - \frac{l_{21}}{l_{22}} \tilde{s}_1 \right) \quad (13)$$

\vdots

$$\tilde{s}_k = \text{mods}_A \left(d_k - \sum_{j < k} \frac{l_{kj}}{l_{kk}} \tilde{s}_j \right), \quad (14)$$

where $\text{mods}_A(x)$ is the symmetric modulo operation that returns the remainder of x after division by A such that $\text{real}(\text{mods}_A(x)) \in [-A/2, A/2)$ and $\text{imag}(\text{mods}_A(x)) \in [-A/2, A/2)$. This modulo operation maintains the transmit

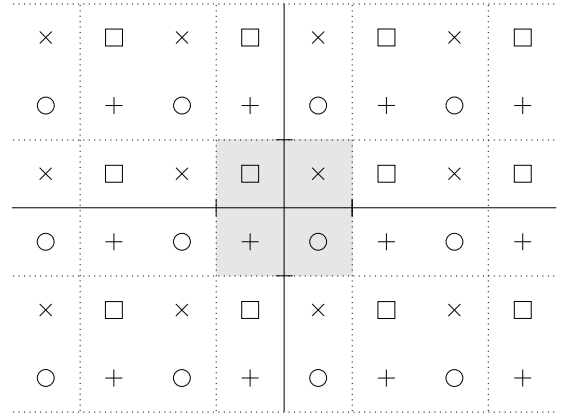


Fig. 2: Expanded constellation points of the 4-QAM in Fig. 1

power of the signal. Then, from (11) the received signal at the k -th user is given by

$$y_k = l_{kk} \tilde{s}_k + \sum_{j < k} l_{kj} \tilde{s}_j + n_k \quad (15)$$

$$= l_{kk} (d_k + c_R A + i c_I A) + n_k, \quad (16)$$

where c_R and c_I are some integers decided by the modulo operation. Here, (16) is valid since $\tilde{s}_k = \text{mods}_A \left(d_k - \sum_{j < k} \frac{l_{kj}}{l_{kk}} \tilde{s}_j \right)$ in (14) can be expressed as $\tilde{s}_k = d_k - \sum_{j < k} \frac{l_{kj}}{l_{kk}} \tilde{s}_j + c_R A + i c_I A$ for some integers c_R and c_I . The processing at the receiver side is rather simple. By dividing the received signal y_k by the effective gain l_{kk} of the k -th user, we can decode the data symbol d_k by using infinitely expanded constellation points shown in Fig. 2. That is, the normalized received signal y_k/l_{kk} is located in a certain shifted box in Fig. 2 and the demodulation of the data symbol d_k is performed in that shifted box. One can see that each user has no other user interference and the power of the transmit signal \tilde{s}_k is similar to the power of the original M -QAM constellation since \tilde{s}_k is contained in the boundary of the original M -QAM constellation shown in Fig. 1 by the modulo operation.

In (10), to apply THP to MU-MISO downlink, we used $\mathbf{Q} = [\mathbf{q}_1, \dots, \mathbf{q}_{N_c}]$ obtained from QR decomposition of \mathbf{H} as the transmit beamforming matrix to make the resulting effective channel matrix as a low-triangular matrix. In fact, to make the resulting effective channel matrix as a low-triangular matrix, we can use any beamforming matrix $\mathbf{W} = [\mathbf{w}_1 \dots \mathbf{w}_{N_c}]$ satisfying the following condition:

$$\mathbf{w}_k \in \mathcal{C}^\perp([\mathbf{h}_1, \mathbf{h}_2, \dots, \mathbf{h}_{(k-1)}]). \quad (17)$$

Hence, the design space for the first user's beam vector \mathbf{w}_1 is the entire space \mathcal{C}^{N_t} , the design space for \mathbf{w}_2 is \mathcal{C}^{N_t-1} , and the design space for the k -th user's beam vector \mathbf{w}_k is \mathcal{C}^{N_t-k} . On the other hand, for the ZF inter-cluster beamforming, the design space for \mathbf{w}_k is $\mathcal{C}^{N_t-N_c+1}$ regardless of k , as seen in (6). When $N_t = N_c$, the beam space for all \mathbf{w}_k is one-dimensional and determined by the channel vectors in the inter-cluster ZF beamforming case. Thus, the dimension of the beam design space is much increased by adopting THP and we can exploit this beam design freedom in addition to

user scheduling to control the ICI to the weak users and to enhance the overall performance in MU-MISO NOMA.

B. Non-Orthogonal Multiple Access with THP

In this subsection, we explain how to apply THP to the considered MU-MISO NOMA downlink system. As aforementioned, in the considered NOMA system, two users in each cluster are chosen so that the strong user has high-quality channel, whereas the weak user is noise-limited. The high-quality channel for the strong user should be maintained for proper operation of NOMA. To be consistent with this design principle of NOMA, we apply THP and design inter-cluster beam vectors so that ICI is eliminated for the strong users. From (1) and (3), the matrix model for the received signals at the strong users at all clusters is given by

$$\mathbf{y}_1 = \mathbf{H}_1^H \mathbf{x} + \mathbf{n}_1 = \mathbf{H}_1^H [\mathbf{w}_1, \dots, \mathbf{w}_{N_c}] \begin{bmatrix} \tilde{x}_1 \\ \vdots \\ \tilde{x}_{N_c} \end{bmatrix} + \mathbf{n}_1, \quad (18)$$

where $\mathbf{y}_1 = [y_{11}, y_{21}, \dots, y_{N_c 1}]^T$, $\mathbf{H}_1 = [\mathbf{h}_{11}, \dots, \mathbf{h}_{N_c 1}]$, and $\mathbf{n}_1 = [n_{11}, n_{21}, \dots, n_{N_c 1}]^T$. Based on the discussion in Section II-A, to apply sequential THP (12) - (14) to the strong users, we require the inter-cluster beam vectors \mathbf{w}_k , $k = 1, \dots, N_c$ to satisfy the following constraint:

$$\mathbf{w}_k \in \mathcal{C}^\perp(\mathbf{H}_1^{<k}), \quad (19)$$

where

$$\mathbf{H}_1^{<k} := [\mathbf{h}_{11} \ \mathbf{h}_{21} \ \dots \ \mathbf{h}_{(k-1)1}] \quad (20)$$

and \mathbf{h}_{k1} is the channel vector from the BS to the strong user in Cluster k . Thus, the dimension of the beam design space for the k -th cluster is $N_t - k + 1$, whereas that of the ZF inter-cluster beamforming is $N_t - N_c + 1$. With the inter-cluster beam vectors $\mathbf{w}_1, \dots, \mathbf{w}_{N_c}$ satisfying (19), we have the signal model for the strong user of Cluster k as

$$y_{k1} = \mathbf{h}_{k1}^H \mathbf{w}_k \tilde{x}_k + \sum_{j=1}^{k-1} \mathbf{h}_{k1}^H \mathbf{w}_j \tilde{x}_j + n_{k1}, \quad (21)$$

which is in the same form as (11). Thus, THP (12) - (14) is applied sequentially to the transmit signal \tilde{x}_k as

$$\tilde{x}_k = \text{mods}_B \left(x_k - \sum_{j < k} \frac{\mathbf{h}_{k1}^H \mathbf{w}_j}{\mathbf{h}_{k1}^H \mathbf{w}_k} \tilde{x}_j \right), \quad (22)$$

where B is the modulo operation factor. Note that THP encoding requires the CSIT of the strong users only. Since we implement NOMA, the signal x_k intended for Cluster k is designed by superposition coding as

$$x_k = \sqrt{p_{k1}} d_{k1} + \sqrt{p_{k2}} d_{k2}, \quad (23)$$

$$p_k = p_{k1} + p_{k2}, \quad \sum_{k=1}^{N_c} p_k \leq P, \quad (24)$$

where d_{k1} and d_{k2} are the modulation data symbols for the strong user and the weak user of the k th cluster, respectively, p_{k1} and p_{k2} are transmit signal power for the strong user

and the weak user of Cluster k , respectively, p_k is the power of Cluster k , and P is the total transmit power of the BS. Note that the modulo-operation in (22) should be performed with an appropriate B by considering the boundary of the super-imposed constellation points. Based on (19) and (22), the received signals (3) and (4) of the strong and weak users of Cluster k are given by

$$\begin{aligned} y_{k1} &= \mathbf{h}_{k1}^H \mathbf{w}_k x_k + n_{k1} \\ y_{k2} &= \mathbf{h}_{k2}^H \mathbf{w}_k \tilde{x}_k + \sum_{j \neq k} \mathbf{h}_{k2}^H \mathbf{w}_j \tilde{x}_j + n_{k2} \\ &= \mathbf{h}_{k2}^H \mathbf{w}_k x_k + \sum_{j < k} \left(\mathbf{h}_{k2}^H \mathbf{w}_j - \frac{\mathbf{h}_{k2}^H \mathbf{w}_k \mathbf{h}_{k1}^H \mathbf{w}_j}{\mathbf{h}_{k1}^H \mathbf{w}_k} \right) \tilde{x}_j \\ &\quad + \sum_{j > k} \mathbf{h}_{k2}^H \mathbf{w}_j \tilde{x}_j + n_{k2}, \end{aligned} \quad (25)$$

where the shifting constants $c_R B + \iota c_I B$ associated with the modulo-operation are omitted in (25) and (26) for simplicity under the assumption that the strong user in Cluster k decodes $x_k = \sqrt{p_{k1}} d_{k1} + \sqrt{p_{k2}} d_{k2}$ based on $y_{k1}/(\mathbf{h}_{k1}^H \mathbf{w}_k)$ and the weak user in Cluster k decodes $x_k = \sqrt{p_{k1}} d_{k1} + \sqrt{p_{k2}} d_{k2}$ based on $y_{k2}/(\mathbf{h}_{k2}^H \mathbf{w}_k)$ by using infinitely expanded constellation points. Precisely, the strong user decodes d_{k2} first and then decodes d_{k1} from the interference-cancelled signal $x_k - \sqrt{p_{k2}} d_{k2}$, whereas the weak user decodes d_{k2} in x_k treating d_{k1} as noise. As seen in (25) and (26), the ICI disappears at the strong user as in the case of ZF inter-cluster beamforming, but the ICI remains at the weak user. However, the components of the received signal at the weak user are different from those of the ZF inter-cluster beamforming case, as seen in (26). The corresponding rates of the strong user and the weak user in Cluster k with the proposed inter-cluster beamforming, THP and SIC are respectively given by[†]

$$R_{k1} = \log_2 \left(1 + \frac{p_{k1} |\mathbf{h}_{k1}^H \mathbf{w}_k|^2}{\sigma^2} \right), \quad (27)$$

$$R_{k2} = \log_2 \left(1 + \min \left\{ \frac{p_{k2} |\mathbf{h}_{k1}^H \mathbf{w}_k|^2}{p_{k1} |\mathbf{h}_{k1}^H \mathbf{w}_k|^2 + \sigma^2}, \frac{p_{k2} |\mathbf{h}_{k2}^H \mathbf{w}_k|^2}{I_k + \sigma^2} \right\} \right) \quad (28)$$

where

$$\begin{aligned} I_k &= p_{k1} |\mathbf{h}_{k2}^H \mathbf{w}_k|^2 + \sum_{j < k} p_j \left| \mathbf{h}_{k2}^H \mathbf{w}_j - \frac{\mathbf{h}_{k2}^H \mathbf{w}_k \mathbf{h}_{k1}^H \mathbf{w}_j}{\mathbf{h}_{k1}^H \mathbf{w}_k} \right|^2 \\ &\quad + \sum_{j > k} p_j |\mathbf{h}_{k2}^H \mathbf{w}_j|^2. \end{aligned} \quad (29)$$

In computation of the strong user rate R_{k1} in (27), the interference from the weak user is not shown since the strong user applies SIC to the interference from the weak user before decoding its own message. The weak user rate R_{k2} is determined by two factors. First, the weak user's data should be decodable at the strong user before decoding the strong user's data at the strong user and the first term in the minimum in (28) represents this rate. Second, the weak user's data should

[†]Here, we neglect the rate loss induced by modulation quantization from the Gaussian input signal. As the order of modulation increases, this quantization loss becomes small. Depending on the SNR, we can select the modulation order adaptively to approach the Gaussian-input rate.

be decodable at the weak user itself, while treating all other signals as noise, and the second term in the minimum in (28) represents this rate. Note that the first term in the RHS of (29) is the interference from the strong user of the same cluster and the second and third terms in the RHS of (29) are ICI. Note that by properly designing the beam vectors we can control the weak user interference I_k in (29) and consequently the weak user rate in (28).

III. PROPOSED USER SCHEDULING AND BEAM DESIGN

In the previous section, we explained how to apply THP to MU-MISO NOMA, and derived the achievable rates of each cluster in the MU-MISO NOMA with THP. In this section, we now tackle the main problem of user scheduling, beam design and power allocation for THP-aided MU-MISO NOMA. In the previous works in which ZF inter-cluster beamforming (6) is considered, the problem of beam design is simple since the ZF constraint (6) determines the beam vectors, and only the problem of user scheduling and power allocation remains. On the contrary, in the case of the considered THP-aided MU-MISO NOMA, we have the further freedom of designing the inter-cluster beam vectors under the relaxed constraint (19) in addition to the freedom of user scheduling and power allocation. There exist several optimality criteria based on the rates of the strong and weak users in (27) and (28). One may consider the maximization of the sum of strong and weak users' rates. However, in the asymmetric channel case where NOMA is meaningful[‡], all cluster power would be allocated to the strong user and this would make the weak user's rate zero, if the criterion of maximization of the sum of strong and weak users' rates were adopted. Hence, one reasonable optimality criterion in this case is to maximize the sum of weak users' rates while guaranteeing certain target rates for the strong users. Thus, under the considered THP-aided MU-MISO NOMA, we consider the optimal beam design and power allocation problem, formulated as follows:

Problem 1: Given total power P and strong user target SNR parameter η , maximize the sum of weak users' rates, i.e.,

$$\max_{R_{k2}, \mathbf{w}_k, p_{k1}, p_{k2}, \forall k} \sum_{k=1}^{N_c} R_{k2} \quad (30)$$

subject to

$$\frac{|\mathbf{h}_{k1}^H \mathbf{w}_k|^2 p_{k1}}{\sigma^2} \geq \eta \frac{P}{N_c} \frac{|\mathbf{\Pi}_{\mathbf{H}_1^{<k}}^\perp \mathbf{h}_{k1}|^2}{\sigma^2}, \quad \forall k \quad (31)$$

$$R_{k2} \leq \log_2 \left(1 + \frac{|\mathbf{h}_{k1}^H \mathbf{w}_k|^2 p_{k2}}{|\mathbf{h}_{k1}^H \mathbf{w}_k|^2 p_{k1} + \sigma^2} \right), \quad \forall k \quad (32)$$

$$R_{k2} \leq \log_2 \left(1 + \frac{|\mathbf{h}_{k2}^H \mathbf{w}_k|^2 p_{k2}}{I_k + \sigma^2} \right), \quad \forall k \quad (33)$$

$$(\mathbf{H}_1^{<k})^H \mathbf{w}_k = \mathbf{0}, \quad \forall k \quad (34)$$

$$\|\mathbf{w}_k\|^2 \leq 1, \quad \forall k \quad (35)$$

$$\sum_k (p_{k1} + p_{k2}) \leq P, \quad (36)$$

[‡]In the case of two-user symmetric channels between strong and weak users, orthogonal multiple access (OMA) is optimal and it achieves the boundary of the capacity region [21].

where I_k is given by (29), $\{\mathbf{h}_{11}, \dots, \mathbf{h}_{N_c1}\}$ are the channel vectors of the scheduled strong users, and $\{\mathbf{h}_{12}, \dots, \mathbf{h}_{N_c2}\}$ are the channel vectors of the scheduled weak users. (Note that in Problem 1, R_{k2} is used as a slack variable and the cost function is linear and hence convex in the overall optimization variables.) Here, the condition (31) is to guarantee a certain target rate for each strong user, where the strong user rate is given by (27). Note that the condition is expressed in terms of SNR. The term $\frac{P}{N_c} |\mathbf{\Pi}_{\mathbf{H}_1^{<k}}^\perp \mathbf{h}_{k1}|^2 / \sigma^2$ in the RHS of (31) represents the nominal maximum SNR for the strong user when \mathbf{w}_k is the matched-filtering beam to \mathbf{h}_{k1} under the THP beam constraint (19). Thus, the target SNR for each strong user is the η -fraction of this nominal maximum SNR. The conditions (32) and (33) implement (28). The condition (34) simply realizes the THP beam constraint (19). The constraints (35) and (36) are power constraints.

The joint design problem of beam design, power allocation and user scheduling under the optimality in Problem 1 is a complicated problem since the rates are dependent not only on the beam design and power allocation but also on user scheduling. To circumvent this difficulty, we apply a three-step approach to the complicated joint problem of beam design, power allocation and user scheduling. The three steps are as follows:

S.1) We first select N_c strong users from the strong user set \mathcal{K}_1 by using the SUS algorithm [16].

S.2) For the set of strong users obtained from Step *S.1*), we then select weak users one by one, while designing the cluster beam vector sequentially under the assumption that equal power is allocated to every cluster.

S.3) Finally, with the selected strong and weak users we solve the problem of beam redesign and power allocation to maximize the performance.

Although the proposed multi-step approach is not an optimal solution to the joint problem of beam design, power allocation and user scheduling, it provides a tractable and efficient solution to the joint problem. It will be shown in Section IV that the proposed method yields noticeable gain over the existing ZF inter-cluster beamforming-based methods. We explain the steps in detail below.

A. User Scheduling via Sequential Greedy Beam Design

The steps *S.1* and *S.2* are basically user scheduling and grouping. User scheduling begins with the selection of N_c strong users from the strong user set \mathcal{K}_1 in Step *S.1*. The initial selection of strong users based only on the channels simplifies the overall problem significantly and such initial separate selection of strong users based on the SUS algorithm was considered in other works as well [9], [13]. For the selection of strong users, even though we use beamforming and THP to eliminate the ICI to the strong users, the strong users with orthogonal channel vectors $\mathbf{h}_{11}, \dots, \mathbf{h}_{N_c1}$ are preferred. This is because in case of orthogonal channel vectors $\mathbf{h}_{11}, \dots, \mathbf{h}_{N_c1}$, by setting $\mathbf{w}_k = \frac{\mathbf{h}_{k1}}{\|\mathbf{h}_{k1}\|}$, there is no ICI and the gain of the resulting individual strong user communication channel is maximized. Furthermore, for NOMA it is better that strong users have high quality channels, which translates to channels

Algorithm 1 User Scheduling with Sequential Beam Design

Step S.1) Strong user selection

- 1: Run the SUS algorithm [16] to select $N_c (\leq N_t)$ users from the strong user set \mathcal{K}_1 .
- 2: Obtain the selected strong users' channels $\mathbf{h}_{11}, \dots, \mathbf{h}_{N_c 1}$.

Step S.2) Weak user selection

- 3: **Initialization:** Given information: $\mathbf{g}_1, \dots, \mathbf{g}_{|\mathcal{K}_2|}$ (user channel vectors in \mathcal{K}_2), P (total power), η (strong user target SNR parameter).

- 4: $p_k = P/N_c$ and $\hat{p}_{k1} = \eta p_k, \forall k$
- 5: $\mathcal{K}_2 \leftarrow \{1, \dots, K_{tot}/2\}$ \triangleright the original weak user set
- 6: \mathcal{S}_1 \triangleright the set of selected strong users from step S.1)
- 7: $\mathcal{S}_2 \leftarrow \phi$ \triangleright the set of selected weak users

$$8: [\hat{\mathbf{w}}_1, \dots, \hat{\mathbf{w}}_{N_c}] = \left[\frac{\mathbf{\Pi}_{\mathbf{H}_{11}^{<k}}^\perp \mathbf{h}_{11}}{\|\mathbf{\Pi}_{\mathbf{H}_{11}^{<k}}^\perp \mathbf{h}_{11}\|}, \dots, \frac{\mathbf{\Pi}_{\mathbf{H}_{N_c 1}^{<k}}^\perp \mathbf{h}_{N_c 1}}{\|\mathbf{\Pi}_{\mathbf{H}_{N_c 1}^{<k}}^\perp \mathbf{h}_{N_c 1}\|} \right]$$

$$9: \mathbf{W} = [],$$

10: Execution:
11: for $k = 1$ to N_c do

12: **(S.2-1)** Compute the rate of every candidate weak user.

13: **for $u = 1$ to $|\mathcal{K}_2|$ do**

$$\begin{aligned} \hat{I}_u = & |\mathbf{g}_u^H \hat{\mathbf{w}}_k|^2 \hat{p}_{k1} + \sum_{j < k} \left| \mathbf{g}_u^H \mathbf{w}_j - \frac{\mathbf{g}_u^H \hat{\mathbf{w}}_k}{\mathbf{h}_{k1}^H \hat{\mathbf{w}}_k} \mathbf{h}_{k1}^H \mathbf{w}_j \right|^2 p_j \\ & + \sum_{j > k} |\mathbf{g}_u^H \hat{\mathbf{w}}_j|^2 p_j, \end{aligned} \quad (37)$$

where \mathbf{w}_l is the l -th column of \mathbf{W} .

14: Compute \hat{R}_u based on (28) with \hat{I}_u and $\hat{\mathbf{w}}_k$.

15: **end for**

16: **(S.2-2)** Select the weak user for cluster k .

17: $u^* = \arg \max_{u \in \mathcal{K}_2} \hat{R}_u$

18: $\mathcal{S}_2 \leftarrow \mathcal{S}_2 \cup \{u^*\}$ and $\mathbf{h}_{k2} \leftarrow \mathbf{g}_{u^*}$

19: $\mathcal{K}_2 \leftarrow \mathcal{K}_2 \setminus \{u^*\}$

20: **(S.2-3)** Greedy beam design:

21: Design \mathbf{w}_k by solving Problem 2.

22: $\mathbf{W} \leftarrow [\mathbf{W}, \mathbf{w}_k]$

23: **end for**

with large channel norms under rough orthogonality. The SUS algorithm is suitable for this purpose because it chooses users with orthogonal channels with large channel norms. We set the N_c strong users returned by the SUS algorithm as the N_c strong users in the N_c clusters (one for each cluster).

After strong user selection, weak users are sequentially selected for each cluster from the weak user set \mathcal{K}_2 by sequentially designing the beam vector for each cluster in a greedy manner under the assumption of equal cluster power allocation. The proposed algorithm is summarized in Algorithm 1. The flow of Algorithm 1 is similar to that of the user scheduling algorithm in [13]. However, Algorithm 1 has several distinctive features relevant to the considered THP-aided MU-MISO NOMA. Note that Algorithm 1 chooses the weak user sequentially from cluster 1 to N_c as seen in Lines 11 to 23 in Algorithm 1. At the time when the weak user is selected and the beam vector is designed for Cluster k ,

the weak users and beam vectors for Cluster $k+1, \dots, N_c$ are not determined yet. However, the beam vector information for Cluster $k+1, \dots, N_c$ is required to compute the ICI in (29), which is required in turn to compute the weak user rate in (28). Hence, we use the matched-filtering beams under the THP beam constraint (19) as the estimates of the undetermined beams for Clusters $k+1, \dots, N_c$, as shown in Line 8 of Algorithm 1. With the already designed beams for Clusters $j < k$ and the beam estimates for Clusters $j \geq k$, the ICI can be estimated as (37), the candidate weak user rate is estimated and the weak user is selected for Cluster k . Then, the beam vector for Cluster k is designed by solving Problem 2, which is a greedy version of our design criterion in Problem 1:

Problem 2:

$$\begin{aligned} & \max_{R_{k2}, \mathbf{w}_k, p_{k1}, p_{k2}} R_{k2} \\ & \text{subject to} \quad \frac{|\mathbf{h}_{k1}^H \mathbf{w}_k|^2 p_{k1}}{\sigma^2} \geq \eta \frac{P}{N_c} \frac{|\mathbf{\Pi}_{\mathbf{H}_{11}^{<k}}^\perp \mathbf{h}_{k1}|^2}{\sigma^2} \\ & R_{k2} \leq \log_2 \left(1 + \frac{|\mathbf{h}_{k1}^H \mathbf{w}_k|^2 p_{k2}}{|\mathbf{h}_{k1}^H \mathbf{w}_k|^2 p_{k1} + \sigma^2} \right) \\ & R_{k2} \leq \log_2 \left(1 + \frac{|\mathbf{h}_{k2}^H \mathbf{w}_k|^2 p_{k2}}{I_k' + \sigma^2} \right) \\ & (\mathbf{H}_1^{<k})^H \mathbf{w}_k = \mathbf{0} \\ & \|\mathbf{w}_k\|^2 \leq 1 \\ & p_{k1} + p_{k2} \leq P/N_c \end{aligned} \quad (38)$$

where

$$\begin{aligned} I_k' = & |\mathbf{h}_{k2}^H \mathbf{w}_k|^2 p_{k1} + \sum_{j < k} \left| \mathbf{h}_{k2}^H \mathbf{w}_j - \frac{\mathbf{h}_{k2}^H \mathbf{w}_k}{\mathbf{h}_{k1}^H \mathbf{w}_k} \mathbf{h}_{k1}^H \mathbf{w}_j \right|^2 \frac{P}{N_c} \\ & + \sum_{j > k} |\mathbf{h}_{k2}^H \hat{\mathbf{w}}_j|^2 \frac{P}{N_c}. \end{aligned} \quad (39)$$

Note that Problem 2 is a non-convex problem. How to solve Problem 2 is discussed in the next subsection.

B. Joint Beam Design and Cluster Power Allocation

In the previous subsection, we considered user scheduling with greedy sequential beam design under the assumption of equal cluster power allocation. Although the sequentially designed beams can be used directly together with the strong and weak users selected by Algorithm 1, it is not optimal under the criterion considered in Problem 1. In this section, we consider the joint beam redesign and power allocation problem, formulated in Problem 1, with the scheduled strong and weak users obtained by Algorithm 1.

Problem 1 is a non-trivial non-convex optimization problem due to the three non-convex constraints (31), (32) and (33). Especially, the ICI term I_k in the decoding of x_2 at the weak user has a complicated form as seen in (29), and hence it is not straightforward how to approach Problem 1. Simple iterative methods may not even guarantee convergence. To solve Problem 1, we resort to SCA [22]. SCA is a method to solve a non-convex optimization problem by iteratively solving properly-constructed approximating convex optimization problems for the original non-convex optimization. It is known that if the approximating convex optimization problems satisfy certain conditions, a stationary point of the original non-convex optimization problem can be obtained by SCA

Algorithm 2 The NOVA Algorithm [22]

Data: Step size $\gamma^{(i)} \in (0, 1]$, initial point $\mathbf{a}^{(0)} \in \mathcal{A}$. Set $i = 0$.
Step 1) If $\mathbf{a}^{(i)}$ is a stationary point of \mathcal{P} (i.e., the cost c_0 does not change any further), stop.
Step 2) Set $\hat{\mathbf{a}}(\mathbf{a}^{(i)})$ as the solution of $\mathcal{P}^{(i)}$.
Step 3) Set $\mathbf{a}^{(i+1)} = \mathbf{a}^{(i)} + \gamma^{(i)}(\hat{\mathbf{a}}(\mathbf{a}^{(i)}) - \mathbf{a}^{(i)})$.
Step 4) $i \leftarrow i + 1$ and go to step 1.

[22]. Below, we summarize the recent result about SCA in [22] as a theorem relevant to Problem 1.

Theorem 1 [22]: Consider a non-convex optimization problem \mathcal{P} with a convex objective function $c_0(\mathbf{a})$ and non-convex constraints $c_l(\mathbf{a}) \leq 0$, $1 \leq l \leq L$, where \mathbf{a} is the optimization variable of \mathcal{P} . Let $\tilde{c}_l(\mathbf{a}, \mathbf{a}^{(i)}) \leq 0$ be the convex constraints approximating the original non-convex constraints $c_l(\mathbf{a}) \leq 0$, where $\mathbf{a}^{(i)}$ is the point for approximation at iteration i , and let the approximating convex optimization problem $\mathcal{P}^{(i)}$ at iteration i be given by the same cost function $c_0(\mathbf{a})$ with $\tilde{c}_l(\mathbf{a}, \mathbf{a}^{(i)}) \leq 0$ replacing $c_l(\mathbf{a}) \leq 0$. Then, if the conditions C1 - C8 below are satisfied, the NOVA algorithm [22] with step-size $\gamma^{(i)}$ satisfying

$$0 < \inf_i \gamma^{(i)} \leq \sup_i \gamma^{(i)} \leq \max_i \gamma^{(i)} \leq 1 \quad (40)$$

yields a stationary point of the problem \mathcal{P} as a limit point.

- C1) c_l are continuously differentiable on \mathcal{U} , where \mathcal{U} is a closed and convex set containing the feasible set \mathcal{A} for \mathcal{P} ;
- C2) $\tilde{c}_l(\bullet; \mathbf{a})$ is convex on \mathcal{U} for all $\mathbf{a} \in \mathcal{A}$.
- C3) $\tilde{c}_l(\mathbf{a}; \mathbf{a}) = c_l(\mathbf{a})$, for all $\mathbf{a} \in \mathcal{A}$;
- C4) $c_l(\mathbf{a}) \leq \tilde{c}_l(\mathbf{a}, \mathbf{b})$ for all $\mathbf{a} \in \mathcal{U}$ and $\mathbf{b} \in \mathcal{A}$;
- C5) $\tilde{c}_l(\bullet; \bullet)$ is continuous on $\mathcal{U} \times \mathcal{A}$;
- C6) $\nabla_{\mathbf{b}} c_l(\mathbf{a}) = \nabla_{\mathbf{b}} \tilde{c}_l(\mathbf{a}; \mathbf{a})$ for all $\mathbf{a} \in \mathcal{A}$;
- C7) $\nabla_{\mathbf{b}} \tilde{c}_l(\bullet; \bullet)$ is continuous on $\mathcal{U} \times \mathcal{A}$.
- C8) The approximating convex optimization problem $\mathcal{P}^{(i)}$ satisfies Slater's condition.

Here, $\nabla_{\mathbf{b}} \tilde{c}_l(\mathbf{a}; \mathbf{a})$ denotes the partial gradient of \tilde{c}_l w.r.t. the its first argument evaluated at \mathbf{a} .

To briefly explain why SCA, specifically the NOVA algorithm works, consider the case of $\gamma^{(i)} = 1$ in (40). Then, the current approximation point $\mathbf{a}^{(i)}$ is the solution of the convex problem $\mathcal{P}^{(i-1)}$. Note that the original problem \mathcal{P} and the approximating convex problem $\mathcal{P}^{(j)}$ for any j have the same convex objective function, and the feasible set of the approximating problem $\mathcal{P}^{(j)}$ for any j is contained in the feasible set of the original problem \mathcal{P} because $\tilde{c}_l(\mathbf{a}, \mathbf{b}) \leq 0$ implies $c_l(\mathbf{a}) \leq 0$ for any \mathbf{a}, \mathbf{b} due to the condition C4. Hence, the solution $\mathbf{a}^{(i)}$ of $\mathcal{P}^{(i-1)}$ is a feasible point of the original problem \mathcal{P} , i.e., $c_l(\mathbf{a}^{(i)}) \leq 0$. Now, consider the new approximating problem $\mathcal{P}^{(i)}$ around $\mathbf{a}^{(i)}$ with constraints $\tilde{c}_l(\mathbf{a}, \mathbf{a}^{(i)}) \leq 0$. By the condition C3 and the fact of $c_l(\mathbf{a}^{(i)}) \leq 0$, we have $\tilde{c}_l(\mathbf{a}^{(i)}, \mathbf{a}^{(i)}) = c_l(\mathbf{a}^{(i)}) \leq 0$. Hence, $\mathbf{a}^{(i)}$ is a point in the feasible set of the new convex problem $\mathcal{P}^{(i)}$. Therefore, the solution $\mathbf{a}^{(i+1)}$ of $\mathcal{P}^{(i)}$ is better (at least not worse) than $\mathbf{a}^{(i)}$ and monotone improvement is achieved by iteration.

Now consider application of Theorem 1 to Problem 1. Since the objective function (30) is linear and the constraints (34), (35) and (36) are convex, we need to convexify the three non-convex constraints (31), (32) and (33) to apply SCA in Theorem 1. The key point of SCA is to obtain proper convex constraints approximating the original non-convex constraints, and this is the major step in SCA. Although direct application of Theorem 1 is not easy due to the complicated structure of (31), (32) and (33), Proposition 1 shows that Problem 1 can be solved with SCA by introducing proper new slack variables, using the first-order Taylor expansion and applying some bounding technique to approximate the original problem to a convex optimization problem.

Proposition 1: Problem 1 can be solved by the proposed iterative algorithm based on SCA, presented in Appendix. The proposed algorithm satisfies the conditions in Theorem 1, which guarantees convergence of the proposed algorithm.

Proof) Here, we briefly provide the sketch of proof. See Appendix for the details.

For convex approximation for Problem 1, we need to convexify the three non-convex constraints (31), (32) and (33). That is, we need to obtain an approximating convex constraint for each of these three non-convex constraints, but more importantly the obtained approximating convex constraints should satisfy the conditions C1 - C8 in Theorem 1 in order to successfully apply SCA to Problem 1. Here, we explain our main techniques for such approximation of the non-convex constraint (31), which is rewritten in the below for convenience:

$$|\mathbf{h}_{k1}^H \mathbf{w}_k|^2 p_{k1} \geq \eta \frac{P}{N_c} |\mathbf{\Pi}_{\mathbf{H}_1^{<k}}^\perp \mathbf{h}_{k1}|^2, \text{ for each } k. \quad (41)$$

The approximation procedures for (32) and (33) are explained in Appendix. The convex approximation procedure for (41) is as follows.

- We first modify the constraint by introducing slack variables to reduce its complexity. Note that the left-hand side (LHS) of (41) is in the form of multiplication of two functions of optimization variables \mathbf{w}_k and p_{k1} , which is complicated to obtain an upper bound that satisfies the condition C4 in Theorem 1. Thus, we first relax this multiplication form by introducing slack variables of exponential forms [23] to exploit the fact that multiplication of exponential functions is the exponential function of the linear sum of their arguments. We introduce $e^{l_{k1}}$ for $|\mathbf{h}_{k1}^H \mathbf{w}_k|^2$ and $e^{m_{k1}}$ for p_{k1} . Then, we have

$$\eta \frac{P}{N_c} |\mathbf{\Pi}_{\mathbf{H}_1^{<k}}^\perp \mathbf{h}_{k1}|^2 \leq e^{l_{k1} + m_{k1}}, \quad (42)$$

$$e^{l_{k1}} \leq p_{k1}, \quad (43)$$

$$e^{m_{k1}} \leq |\mathbf{h}_{k1}^H \mathbf{w}_k|^2 (= \mathbf{w}_k^H (\mathbf{h}_{k1} \mathbf{h}_{k1}^H) \mathbf{w}_k). \quad (44)$$

Note that the LHS of (41) is converted to a simple exponential function of the linear sum of two slack variables in (42). To compensate for this substitution, eqs. (43) and (44) are newly added. The directions of the inequalities are determined to be consistent with the original constraint (41). The resulting new three constraints (42), (43) and (44) implementing (41) are in the form of (a convex function \leq a convex function). (43) is

already a convex constraint since the larger side of (43) is a linear function.

- Note that the desired constraint form in Theorem 1 is (a convex function ≤ 0) and the difference of two strictly convex functions as shown in (42) and (44) is not convex. Thus, we need to process (42) and (44) further. By obtaining a linear lower-bound for the larger side of each inequality, we can approximate the constraint to a convex constraint. For this, we use the first-order Taylor expansion. By applying the first-order Taylor expansion to the larger side of each of (42) and (44) at the current point $(\bar{l}_{k1}, \bar{m}_{k1}, \bar{\mathbf{w}}_k)$, which corresponds to $\mathbf{a}^{(i)}$ in Theorem 1, (42) and (44) are approximated to two convex constraints satisfying C2 in Theorem 1:

$$\eta \frac{P}{N_c} |\mathbf{\Pi}_{\mathbf{H}_1^{\perp}} \mathbf{h}_{k1}|^2 \leq e^{\bar{l}_{k1} + \bar{m}_{k1}} (1 + l_{k1} + m_{k1} - \bar{l}_{k1} - \bar{m}_{k1}), \quad (45)$$

$$e^{m_{k1}} \leq |\mathbf{h}_{k1}^H \bar{\mathbf{w}}_k|^2 + \langle \mathbf{h}_{k1} \mathbf{h}_{k1}^H \bar{\mathbf{w}}_k, \mathbf{w}_k - \bar{\mathbf{w}}_k \rangle. \quad (46)$$

where $\langle \mathbf{a}, \mathbf{b} \rangle = 2\text{Re}(\mathbf{a}^H \mathbf{b})$. Note that for a given convex function, the first-order Taylor expansion is a linear lower bound of the convex function and it has the same function value and gradient value as the original function at the point of expansion. Since the first-order Taylor expansion was applied to the larger side of the inequality, the obtained approximating convex constraints satisfy the conditions C3, C4, C6 in Theorem 1.[§] In addition, it is easy to check the validity of the continuity and differentiability conditions C1, C5, C7 in Theorem 1.

- We can approximate (32) and (33) with convex constraints by applying similar techniques, but additional techniques are necessary to simplify (33) due to the complexity of I_k shown in (29). Basically, I_k is too complicated for convex approximation. Although convex approximation with the exact I_k is possible, it leads to a complicated convex problem with too many slack variables. Hence, we use an upper bound of I_k and compute the lower bound of the second term in the minimum in (28) for R_{k2} . Then, we maximize this lower bound of R_{k2} . The details of convex approximations of (32) and (33) are in Appendix.

- The point used for the first-order Taylor expansion is the approximation point $\mathbf{a}^{(i)}$ in Theorem 1. We can iteratively update the approximation point $\mathbf{a}^{(i)}$ by using the solution of the approximating convex optimization problem like the NOVA algorithm in Theorem 1. In this way, we obtain a sequence of solutions of the approximating convex problems, which converges to a stationary point of Problem 1 with R_{k2} replaced by the above-mentioned lower bound by Theorem 1, since the approximating constraints satisfy the conditions in Theorem 1. ■

Problem 2 is a simpler version of Problem 1, and hence it can be solved in a similar way.

[§]That is, each non-convex constraint is in the form of $c_{l,L}(\mathbf{a}) \leq c_{l,U}(\mathbf{a})$, i.e., $c_l(\mathbf{a}) := c_{l,L}(\mathbf{a}) - c_{l,U}(\mathbf{a}) \leq 0$ with $c_{l,L}, c_{l,U}$ convex. Let $t_l(\mathbf{a}, \mathbf{a}^{(i)})$ be the first-order Taylor expansion of $c_{l,U}(\mathbf{a})$ at $\mathbf{a}^{(i)}$. Then, $t_l(\mathbf{a}, \mathbf{a}^{(i)}) \leq c_{l,U}(\mathbf{a})$ and $t_l(\mathbf{a}^{(i)}, \mathbf{a}^{(i)}) = c_{l,U}(\mathbf{a}^{(i)})$. Hence, we set the approximating convex constraint as $\tilde{c}_l(\mathbf{a}, \mathbf{a}^{(i)}) := c_{l,L}(\mathbf{a}) - t_l(\mathbf{a}, \mathbf{a}^{(i)}) \leq 0$, which satisfies C3, C4, C6 in Theorem 1.

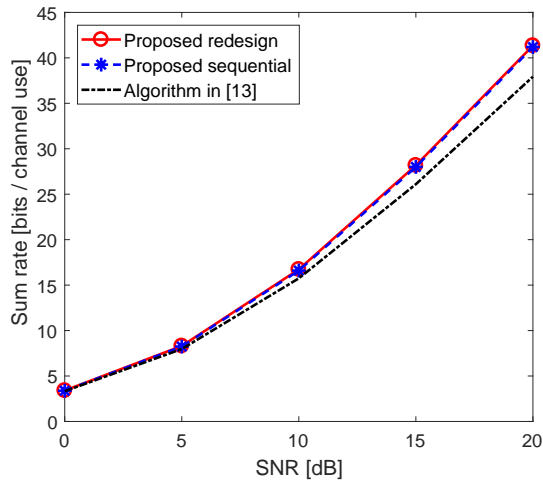
IV. NUMERICAL RESULTS

In this section, we provide some numerical results to evaluate the performance of the proposed user scheduling, beam design and power allocation algorithm for MU-MISO NOMA downlink. The basic setting for the simulations in this section is as follows: The AWGN variance was set to be one, i.e., $\sigma^2 = 1$ throughout the simulations. Each element of the channel vector for each strong user in \mathcal{K}_1 was generated independently from $\mathcal{CN}(0, \sigma_{h,1}^2)$ with $\sigma_{h,1}^2 = 1$, whereas each element of the channel vector for each weak user in \mathcal{K}_2 was generated independently from $\mathcal{CN}(0, \sigma_{h,2}^2)$ with $\sigma_{h,2}^2 = 0.01$. Hence, we have 20 dB difference in channel quality between the strong and weak users. ($|\mathcal{K}_1| = |\mathcal{K}_2| = K_{tot}/2$.)

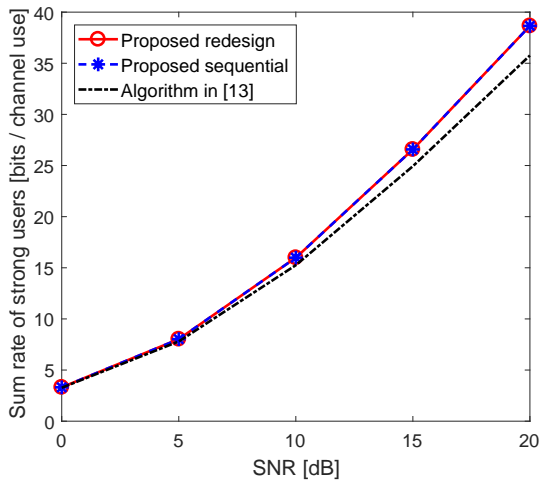
As the comparison baseline, we considered several hierarchical design methods for MU-MISO NOMA, the design method in [13], the NOMA-ZFBF-UMPS algorithm in [9], and the NOMA-FOUS algorithm in [12]. The design method in [13] is based on ZF inter-cluster beamforming and uses the two-user Pareto-optimal beam design and power allocation for the strong and weak users in each cluster forming a MISO broadcast channel with superposition coding and SIC. Thus, the intra-cluster design used in this method is optimal in the Pareto-optimality sense. For each cluster this method sets a certain target SNR for the strong user and maximizes the weak user rate. Hence, this method has the capability of trading off the strong user rate for the weak user rate by changing the target SNR for the strong user. It is shown in [13] that this method outperforms several other user scheduling and power allocation method based on ZF inter-cluster beamforming. The original algorithms in [12], [9] consider only a single set of users for selection of both strong and weak users. Hence, the simulation setting in [12], [9] is different. So, we modified the original two algorithms to make the strong user be selected from \mathcal{K}_1 and the weak user be selected from \mathcal{K}_2 .

Fig. 3 shows the performance of the proposed THP-aided algorithm as compared to the ZF intercluster-beamforming-based method in [13]. The figure shows the average rate versus SNR defined as $10 \log_{10} \frac{P}{\sigma^2}$ for $N_t = 8$, $K_{tot} = 200$ (i.e., $|\mathcal{K}_1| = |\mathcal{K}_2| = 100$). The value of the strong user target SNR parameter η was set as $\eta = 0.3$ for the proposed method, whereas $\eta = 0.4$ (this second η as defined in [13]) for the ZF intercluster-beamforming-based method in [13]. (The definition of η in [13] is a bit different from that in this paper, but the role is the same.) The average rates were obtained by averaging 50 independent channel realizations. It is seen that the proposed THP-aided method outperforms the ZF intercluster beamforming-based method in [13]. It is also seen that the beam redesign and power allocation by solving Problem 1 yields non-trivial gain over the initial sequential greedy beam design with equal cluster power allocation in Section III-A.

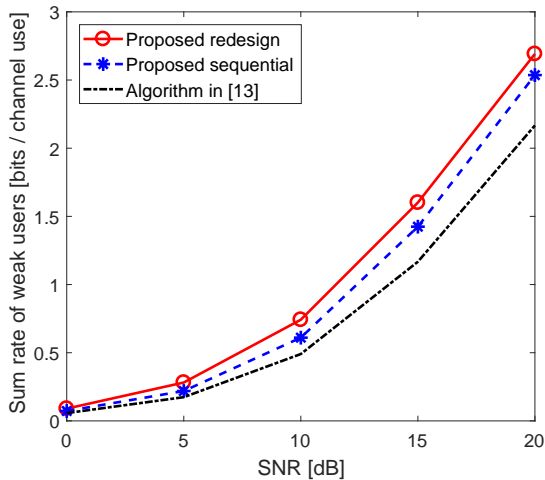
Fig. 4 shows the sum strong user rate versus the sum weak user rate by sweeping the strong user target SNR parameter η in Problem 1 for $N_t = 8$, $|\mathcal{K}_1| = |\mathcal{K}_2| = 100$, and $10 \log_{10} \frac{P}{\sigma^2} = 15$ dB. Note that the algorithm in [13] has the capability of trading off the strong user rate for the weak user rate, whereas the NOMA-ZFBF-UMPS algorithm and the



(a)



(b)



(c)

Fig. 3: The average rate versus $10 \log_{10}(P/\sigma^2)$ ($N_t = 8$, $K_{tot} = 200$): (a) total sum rate, (b) sum rate of strong users, and (c) sum rate of weak users

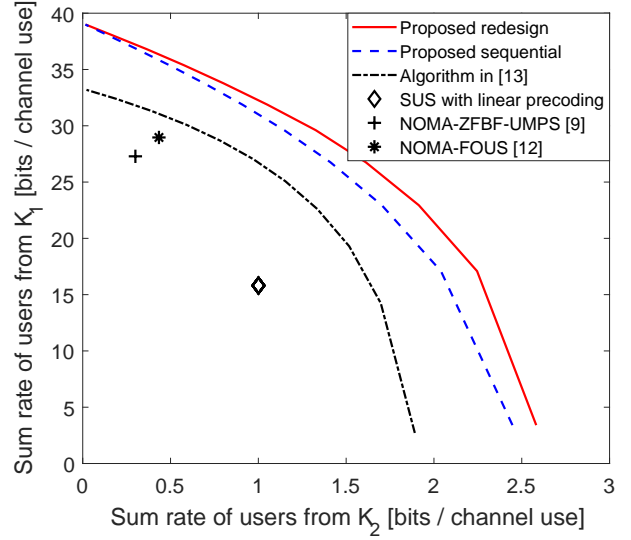


Fig. 4: Sum strong user rate versus sum weak user rate with sweeping η ($N_t = 8$, $|\mathcal{K}_1| = |\mathcal{K}_2| = 100$, and $10 \log_{10} \frac{P}{\sigma^2} = 15$ dB)

NOMA-FOUS algorithm do not. It is seen that the proposed THP-based method enlarges the rate region noticeably as compared to the existing ZF intercluster beamforming-based methods. Again, it is seen that the beam redesign and power allocation by solving Problem 1 yields non-trivial gain over the initial sequential greedy beam design with equal cluster power allocation in Section III-A.

V. CONCLUSION

In this paper, we have considered THP for MU-MISO NOMA downlink systems. We have applied THP under the hierarchical structure in which multiple clusters each with two users are formed and served in the spatial domain and users in each cluster are served in the power domain. The application of THP eliminates ICI to the strong users and enlarges the dimension of the beam design space, which can be exploited for inter-cluster beam design to mitigate ICI to weak users on top of weak user selection. Exploiting this enlarged beam design space, we have proposed a two-step user scheduling algorithm together with two beam design methods: sequential greedy beam design and after-user-selection beam redesign and power allocation. To solve the design problems, we have proposed an efficient algorithm based on SCA, which guarantees convergence to a stationary point of the problem. Numerical results show that the proposed THP-aided beam design and user scheduling yield noticeable gain over existing ZF inter-cluster beamforming-based methods. Furthermore, the introduced two-step technique for convexification for SCA can be useful to other general problems requiring convex approximation.

APPENDIX

Proof of Proposition 1: Since in Problem 1 the objective function (30) is linear and the constraints (34), (35) and

(36) are convex, we need to obtain approximating convex constraints for the three non-convex constraints (31), (32) and (33) satisfying the conditions C1 - C8 in Theorem 1. Then, we can apply the NOVA algorithm to obtain a stationary point of Problem 1.

The non-convex constraints (31), (32) and (33) of Problem 1 are rewritten here for convenience as

$$|\mathbf{h}_{k1}^H \mathbf{w}_k|^2 p_{k1} \geq \eta \frac{P}{N_c} |\mathbf{\Pi}_{\mathbf{H}_k}^\perp \mathbf{h}_{k1}|^2, \quad (47)$$

$$R_{k2} \leq \log_2 \left(1 + \frac{|\mathbf{h}_{k1}^H \mathbf{w}_k|^2 p_{k2}}{|\mathbf{h}_{k1}^H \mathbf{w}_k|^2 p_{k1} + \sigma^2} \right), \quad (48)$$

$$R_{k2} \leq \log_2 \left(1 + \frac{|\mathbf{h}_{k2}^H \mathbf{w}_k|^2 p_{k2}}{I_k + \sigma^2} \right), \quad (49)$$

where

$$I_k = |\mathbf{h}_{k2}^H \mathbf{w}_k|^2 p_{k1} + \sum_{j < k} \left| \mathbf{h}_{k2}^H \mathbf{w}_j - \frac{\mathbf{h}_{k2}^H \mathbf{w}_k}{\mathbf{h}_{k1}^H \mathbf{w}_k} \mathbf{h}_{k1}^H \mathbf{w}_j \right|^2 p_j + \sum_{j > k} |\mathbf{h}_{k2}^H \mathbf{w}_j|^2 p_j. \quad (50)$$

Step 1) First, we convert the three non-convex constraints into the form of (a convex function \leq a convex function) by introducing slack variables $\bigcup_{k=1}^{N_c} \{m_{k1}, m_{k2}, m_{k3}, l_{k1}, l_{k2}, l_{k3}, l_{k4}, n_{kj} \ \forall j \neq k\}$ as follows:

$$i) |\mathbf{h}_{k1}^H \mathbf{w}_k|^2 p_{k1} \geq \eta \frac{P}{N_c} |\mathbf{\Pi}_{\mathbf{H}_k}^\perp \mathbf{h}_{k1}|^2 \text{ (eq.(47))} :$$

$$e^{l_{k1} + m_{k1}} \geq \eta \frac{P}{N_c} |\mathbf{\Pi}_{\mathbf{H}_k}^\perp \mathbf{h}_{k1}|^2, \quad (51)$$

$$e^{l_{k1}} \leq p_{k1}, \quad (52)$$

$$e^{m_{k1}} \leq |\mathbf{h}_{k1}^H \mathbf{w}_k|^2, \quad (53)$$

$$ii) R_{k2} \leq \log_2 \left(1 + \frac{|\mathbf{h}_{k1}^H \mathbf{w}_k|^2 p_{k2}}{|\mathbf{h}_{k1}^H \mathbf{w}_k|^2 p_{k1} + \sigma^2} \right) \text{ (eq. (48))}:$$

$$(2^{R_{k2}} - 1) \cdot (\sigma^2 + e^{l_{k2} + m_{k1}}) \leq e^{l_{k3} + m_{k1}}, \quad (54)$$

$$e^{l_{k2}} \geq p_{k1}, \quad (55)$$

$$e^{l_{k3}} \leq p_{k2}, \quad (56)$$

where (54) can further be changed in the form of (a convex function \leq a convex function) as

$$\sigma^2 2^{R_{k2}} + 2^{R_{k2}} e^{l_{k2} + m_{k1}} \leq \sigma^2 + e^{l_{k2} + m_{k1}} + e^{l_{k3} + m_{k1}}. \quad (57)$$

The procedure for *i)* is already explained in the below of Proposition 1, and a similar procedure is applied to *ii)*.

iii) $R_{k2} \leq \log_2 \left(1 + \frac{|\mathbf{h}_{k2}^H \mathbf{w}_k|^2 p_{k2}}{I_k + \sigma^2} \right)$ (eq. (49)): Convex approximation of this constraint is complicated due to the structure of I_k as shown in (50). The first and third terms in the RHS of (50) are in the form of the product of a power term and a quadratic term of \mathbf{w}_k , but the second term of the RHS of (50) is not simple. Although convex approximation with the exact I_k is possible, this leads to a complicated convex problem with too many slack variables. Hence, we use an upper bound of

the second term of the RHS of (50) to simplify the problem. The second term of the RHS of (50) can be upper bounded as

$$\begin{aligned} & \left| \mathbf{h}_{k2}^H \mathbf{w}_j - \frac{\mathbf{h}_{k2}^H \mathbf{w}_k}{\mathbf{h}_{k1}^H \mathbf{w}_k} \mathbf{h}_{k1}^H \mathbf{w}_j \right|^2 p_j \\ &= \frac{|\mathbf{h}_{k1}^H \mathbf{w}_k \cdot \mathbf{h}_{k2}^H \mathbf{w}_j - \mathbf{h}_{k2}^H \mathbf{w}_k \cdot \mathbf{h}_{k1}^H \mathbf{w}_j|^2 p_j}{|\mathbf{h}_{k1}^H \mathbf{w}_k|^2} \end{aligned} \quad (58)$$

$$\stackrel{(a)}{\leq} \frac{(|\mathbf{h}_{k1}^H \mathbf{w}_k|^2 + |\mathbf{h}_{k2}^H \mathbf{w}_k|^2) \cdot (|\mathbf{h}_{k1}^H \mathbf{w}_j|^2 + |\mathbf{h}_{k2}^H \mathbf{w}_j|^2) p_j}{|\mathbf{h}_{k1}^H \mathbf{w}_k|^2} \quad (59)$$

$$= \frac{\mathbf{w}_k^H (\mathbf{h}_{k1} \mathbf{h}_{k1}^H + \mathbf{h}_{k2} \mathbf{h}_{k2}^H) \mathbf{w}_k \cdot \mathbf{w}_j^H (\mathbf{h}_{k1} \mathbf{h}_{k1}^H + \mathbf{h}_{k2} \mathbf{h}_{k2}^H) \mathbf{w}_j p_j}{|\mathbf{h}_{k1}^H \mathbf{w}_k|^2} \quad (60)$$

where the Cauchy-Schwartz inequality is applied to step (a). By summing the term in (60) and the first and third terms in the RHS of (50), we have an upper bound, denoted by \tilde{I}_k , on I_k . Substituting \tilde{I}_k into I_k yields a lower bound on R_{k2} . Hence, by approximating (49) with \tilde{I}_k instead of I_k , we modify the original problem, Problem 1, slightly as the problem of maximizing the lower bound of $\sum_k R_{k2}$. (Note that a lower bound is taken only on the second term of the RHS of (28).) Since $\mathbf{\Pi}_k := \mathbf{h}_{k1} \mathbf{h}_{k1}^H + \mathbf{h}_{k2} \mathbf{h}_{k2}^H$ in the numerator of (60) is a positive-definite matrix, we can substitute the terms p_j , $\mathbf{w}_k^H \mathbf{\Pi}_k \mathbf{w}_k$, $\mathbf{w}_j^H \mathbf{\Pi}_k \mathbf{w}_j$ and $|\mathbf{h}_{k1}^H \mathbf{w}_k|^2$ in (60) by exponential functions with new slack variables. Then, the constraint (49) with I_k replaced by \tilde{I}_k is rewritten as

$$(2^{R_{k2}} - 1) \cdot (\tilde{I}_k + \sigma^2) \leq e^{l_{k3} + m_{k2}}, \quad (61)$$

$$e^{m_{k2}} \leq |\mathbf{h}_{k2}^H \mathbf{w}_k|^2, \quad (62)$$

$$e^{m_{k3}} \geq \mathbf{w}_k^H (\mathbf{h}_{k1} \mathbf{h}_{k1}^H + \mathbf{h}_{k2} \mathbf{h}_{k2}^H) \mathbf{w}_k, \quad (63)$$

$$e^{l_{k4}} \geq p_k \quad (\text{i.e., } e^{l_{j4}} \geq p_j), \quad (64)$$

$$e^{n_{kj}} \geq \begin{cases} \mathbf{w}_j^H (\mathbf{h}_{k1} \mathbf{h}_{k1}^H + \mathbf{h}_{k2} \mathbf{h}_{k2}^H) \mathbf{w}_j, & \text{for } j < k, \\ |\mathbf{h}_{k2}^H \mathbf{w}_j|^2, & \text{for } j > k \end{cases} \quad (65)$$

where

$$\tilde{I}_k = e^{l_{k2} + m_{k2}} + e^{m_{k3} - m_{k1}} \sum_{j < k} e^{l_{j4} + n_{kj}} + \sum_{j > k} e^{l_{j4} + n_{kj}}. \quad (66)$$

Note that the directions of the inequalities with the newly introduced slack variables are determined to maintain consistency with the original non-convex optimization.

Step 2) In Step 1, by introducing the slack variables, we expressed the three non-convex constraints as multiple inequalities each in the form of $c_{l,L}(\mathbf{a}) \leq c_{l,U}(\mathbf{a})$, i.e., $c_l(\mathbf{a}) := c_{l,L}(\mathbf{a}) - c_{l,U}(\mathbf{a}) \leq 0$, with $c_{l,L}, c_{l,U}$ convex in the optimization variables \mathbf{a} . To obtain the desired form of the approximating convex constraint described in Theorem 1, we apply the first-order Taylor expansion to the larger side of each of the inequality constraints obtained in Step 1 at the current point of Taylor expansion, which corresponds to $\mathbf{a}^{(i)}$ in Theorem 1. That is, let $t_l(\mathbf{a}, \mathbf{a}^{(i)})$ be the first-order Taylor expansion of $c_{l,U}(\mathbf{a})$ at $\mathbf{a}^{(i)}$. Then, $t_l(\mathbf{a}, \mathbf{a}^{(i)}) \leq c_{l,U}(\mathbf{a})$ and $t_l(\mathbf{a}^{(i)}, \mathbf{a}^{(i)}) = c_{l,U}(\mathbf{a}^{(i)})$ since the first-order Taylor expansion for a given convex function is a linear lower bound of the convex function and has the same function value as the original function at the point of expansion. Furthermore,

it has the same gradient value as the original function at the point of expansion. Hence, we obtain a desired approximating convex constraint as $\tilde{c}_l(\mathbf{a}, \mathbf{a}^{(i)}) := c_{l,L}(\mathbf{a}) - t_l(\mathbf{a}, \mathbf{a}^{(i)}) \leq 0$ for each $c_l(\mathbf{a}) = c_{l,L}(\mathbf{a}) - c_{l,U}(\mathbf{a}) \leq 0$. Then, the approximating convex constraints satisfy C3, C4, C6 as well as the easily-verifiable continuity and differentiability conditions C1, C5, C7 in Theorem 1. Thus, we finally obtain a convex optimization problem approximating Problem 1 with I_k replaced by \bar{I}_k , given by $\mathcal{P}_1(\bar{\alpha})$ in the next page. In $\mathcal{P}_1(\bar{\alpha})$,

$$\bar{\alpha} := [\{\bar{\mathbf{w}}_k, \bar{m}_{k1}, \bar{m}_{k2}, \bar{m}_{k3}, \bar{l}_{k1}, \bar{l}_{k2}, \bar{l}_{k3}, \bar{l}_{k4}, \bar{n}_{kj} \forall j \neq k\}_{k=1}^{N_c}]$$

is the point at which the first-order Taylor series is obtained, and

$$f(x, \bar{x}) := e^{\bar{x}}(1 + x - \bar{x}), \quad (67)$$

$$g_{\mathbf{c}}(\mathbf{d}, \bar{\mathbf{d}}) := |\mathbf{c}^H \bar{\mathbf{d}}|^2 + \langle \mathbf{c} \mathbf{c}^H \bar{\mathbf{d}}, \mathbf{d} - \bar{\mathbf{d}} \rangle, \quad (68)$$

where $\langle \mathbf{c}, \mathbf{d} \rangle = 2\text{Re}(\mathbf{c}^H \mathbf{d})$. (These two functions are the first-order Taylor series of $\tilde{f}(x) := e^x$ at \bar{x} and $\tilde{g}_{\mathbf{c}}(\mathbf{d}) := |\mathbf{c}^H \mathbf{d}|^2$ at $\bar{\mathbf{d}}$, respectively.)

In $\mathcal{P}_1(\bar{\alpha})$, (72)-(74) correspond to (47); (75)-(77) correspond to (48); and (78)-(81) and (74) with $q = 2$ correspond to (49). Since $\mathcal{P}_1(\bar{\alpha})$ is a convex problem, it can be solved by any convex optimization solver.

Step 3) Now, we propose an algorithm that iteratively solves $\mathcal{P}_1(\bar{\alpha})$ by updating its parameter vector $\bar{\alpha}$. Let $\bar{\alpha}^{(i)}$ be the Taylor expansion parameter vector at iteration i , given by

$$\bar{\alpha}^{(i)} := [\{\bar{\mathbf{w}}_k^{(i)}, \bar{m}_{k1}^{(i)}, \bar{m}_{k2}^{(i)}, \bar{m}_{k3}^{(i)}, \bar{l}_{k1}^{(i)}, \bar{l}_{k2}^{(i)}, \bar{l}_{k3}^{(i)}, \bar{l}_{k4}^{(i)}, \bar{n}_{kj}^{(i)} \forall j \neq k\}_{k=1}^{N_c}]. \quad (69)$$

The proposed algorithm is basically an application of the NOMA algorithm [22] shown in Algorithm 2. The proposed algorithm is summarized in Algorithm 3. In line 7 of Algorithm 3, for the update of the Taylor expansion point, we used the setting that corresponds to $\gamma^{(i)} = 1$ in Step 3 of the NOVA algorithm shown in Algorithm 2. We initialize $\bar{\alpha}^{(0)}$ as follows: First, with the convexification techniques in Steps 1 and 2, we solve the simpler sequential problem, Problem 2 with initialization of $p_{k1}^{(0)}, p_{k2}^{(0)}$, and $\mathbf{w}_k^{(0)}$ as in lines 3 - 8 in

Algorithm 1 together with slack variable initialization:

$$\begin{aligned} \bar{m}_{kq}^{(0)} &= \log(|\mathbf{h}_{kq}^H \mathbf{w}_k^{(0)}|^2), \text{ for } q = 1, 2, \\ \bar{m}_{k3}^{(0)} &= \log((\mathbf{w}_k^{(0)})^H (\mathbf{h}_{k1} \mathbf{h}_{k1}^H + \mathbf{h}_{k2} \mathbf{h}_{k2}^H) \mathbf{w}_k^{(0)}), \\ \bar{l}_{k1}^{(0)} &= \bar{l}_{k2}^{(0)} = \log(p_{k1}^{(0)}), \\ \bar{l}_{k3}^{(0)} &= \log(p_{k2}^{(0)}), \\ \bar{l}_{k4}^{(0)} &= \log(p_k^{(0)}), \\ \bar{n}_{kj}^{(0)} &= \begin{cases} \log((\mathbf{w}_j^{(0)})^H (\mathbf{h}_{k1} \mathbf{h}_{k1}^H + \mathbf{h}_{k2} \mathbf{h}_{k2}^H) \mathbf{w}_j^{(0)}), & \forall j < k \\ \log(|\mathbf{h}_{k2}^H \mathbf{w}_j^{(0)}|^2) & \forall j > k. \end{cases} \end{aligned} \quad (70)$$

Then, with the obtained solution from Problem 2, we initialize $p_{k1}^{(0)}, p_{k2}^{(0)}$, and $\mathbf{w}_k^{(0)}$ for Problem 1 and slack variables for Problem 1 with the same way as in (70).

Step 4) Finally, we prove that Algorithm 3 converges to a stationary point of Problem 1 with I_k replaced by \bar{I}_k . It is already mentioned in Step 2 that the obtained approximating convex problem satisfies the conditions C1-C7 of Theorem 1. The final technical condition in Theorem 1 is Slater's condition C8. Note that Slater's condition requires that there exists an interior feasible point, i.e., a feasible point that satisfies every inequality constraint of the problem with strict inequality. We can state that if $\mathcal{P}_1(\bar{\alpha}^{(i)})$ has a non-trivial solution such that $\sum_k R_{k2} \neq 0$, then there exists an interior feasible point for $\mathcal{P}_1(\bar{\alpha}^{(i)})$. Consider the solution of $\mathcal{P}_1(\bar{\alpha}^{(i)})$, $\mathcal{S}^{(i)} = \{R_{k2}^{(i)*}, \mathbf{w}^{(i)*}, p_{k1}^{(i)*}, p_{k2}^{(i)*}, \forall k$ and slack variables $\}^*$. By setting $R_{k2}^{(i)*} = 0, \forall k$ and fixing other variables in $\mathcal{S}^{(i)}$, the constraints (75) and (78) involving R_{k2} are satisfied with strict inequality. By exploiting the gap between the LHS and RHS of (75) and (78), we can adjust other variables in $\mathcal{S}^{(i)}$ to have strict inequality for all other constraints. That is, since $R_{k2}^{(i)*}$ is decreased, every slack variable related to interference such as l_{k2}, l_{k4}, m_{k3} and n_{kj} for $j \neq k$, can be increased while strict inequality for (75) and (78) is remained. Then, the constraints inserted by introducing these slack variables satisfy strict inequality. Other slack variables can be adjusted with sufficiently small amount to have strict inequality for the remaining constraints. Thus, there exists a set of variables that satisfy all the constraints with strict inequality if $\mathcal{P}_1(\bar{\alpha}^{(i)})$ has a non-trivial solution such that $\sum_k R_{k2} \neq 0$.

Therefore, by Theorem 1, the proposed algorithm converges to a stationary point of Problem 1 with I_k replaced by \bar{I}_k . ■

REFERENCES

- [1] G. T. 36.859, "Study on downlink multiuser superposition transmission," *3GPP*, 2015.
- [2] Y. Saito, Y. Kishiyama, A. Benjebbour, T. Nakamura, A. Li, and K. Higuchi, "Non-orthogonal multiple access (NOMA) for cellular future radio access," in *Proc. IEEE VTC Spring*, pp. 1-5, Jun. 2013.
- [3] Z. Ding, Z. Yang, P. Fan, and H. V. Poor, "On the performance of non-orthogonal multiple access in 5G systems with randomly deployed users," *IEEE Trans. Signal Process.*, vol. 21, pp. 1501-1505, Jul. 2014.
- [4] S. Timotheou and I. Krikidis, "Fairness for non-orthogonal multiple access in 5G systems," *IEEE Signal Process. Lett.*, vol. 22, pp. 1647-1651, Mar. 2015.
- [5] F. Liu, P. Mähönen, and M. Petrova, "Proportional fairness-based user pairing and power allocation for non-orthogonal multiple access," in *Proc. IEEE PIMRC* pp. 1127-1131, Aug. 2015.

Algorithm 3 Joint Beam Design and Power Allocation

- 1: **Initialization:**
 - 2: Initialize $\bar{\alpha}^{(0)}$.
 - 3: Set the stopping parameter ϵ .
 - 4: $i \leftarrow 0, R_{k2}^{(-1)} \leftarrow 0, R_{k2}^{(-2)} \leftarrow 0, \forall k$.
 - 5: **while** $i = 0$ or $(\sum_k R_{k2}^{(i-1)} - \sum_k R_{k2}^{(i-2)}) < \epsilon$ **do**
 - 6: Solve $\mathcal{P}_1(\bar{\alpha}^{(i)})$ and obtain its solution $\mathcal{S}^{(i)}$.
 - 7: Update $\bar{\alpha}^{(i+1)}$ with $\mathcal{S}^{(i)}$.
 - 8: $i \leftarrow i + 1$
 - 9: **end while**
-

$\mathcal{P}_1(\bar{\alpha})$: The Approximated Convex Problem

$$\max_{R_{k2}, \mathbf{w}_k, p_{k1}, p_{k2}, \forall k, \text{ and slack variables}} \sum_k R_{k2} \quad (71)$$

subject to

$$f(l_{k1} + m_{k1}, \bar{l}_{k1} + \bar{m}_{k1}) \geq \eta \frac{P}{N_c} |\mathbf{\Pi}_{\mathbf{H}_k}^\perp \mathbf{h}_{k1}|^2, \quad \forall k \quad (72)$$

$$e^{l_{k1}} \leq p_{k1}, \quad \forall k \quad (73)$$

$$e^{m_{kq}} \leq g_{\mathbf{h}_{kq}}(\mathbf{w}_k, \bar{\mathbf{w}}_k), \quad \forall k, \quad q = 1, 2 \quad (74)$$

$$e^{R_{k2} \ln 2 + l_{k2} + m_{k1}} + \sigma^2 e^{R_{k2} \ln 2} \leq \sigma^2 + f(l_{k2} + m_{k1}, \bar{l}_{k2} + \bar{m}_{k1}) + f(l_{k3} + m_{k1}, \bar{l}_{k3} + \bar{m}_{k1}), \quad \forall k \quad (75)$$

$$f(l_{k2}, \bar{l}_{k2}) \geq p_{k1}, \quad \forall k \quad (76)$$

$$e^{l_{k3}} \leq p_{k2}, \quad \forall k \quad (77)$$

$$e^{R_{k2} \ln 2 (\tilde{I}_k + \sigma^2)} \leq \sigma^2 + f(l_{k2} + m_{k2}, \bar{l}_{k2} + \bar{m}_{k2}) + \sum_{j < k} f(m_{k3} - m_{k1} + l_{j4} + n_{kj}, \bar{m}_{k3} - \bar{m}_{k1} + \bar{l}_{j4} + \bar{n}_{kj}) + \sum_{j > k} f(l_{j4} + n_{kj}, \bar{l}_{j4} + \bar{n}_{kj}) + f(l_{k3} + m_{k2}, \bar{l}_{k3} + \bar{m}_{k2}), \quad \forall k \quad (78)$$

$$f(m_{k3}, \bar{m}_{k3}) \geq \mathbf{w}_k^H (\mathbf{h}_{k1} \mathbf{h}_{k1}^H + \mathbf{h}_{k2} \mathbf{h}_{k2}^H) \mathbf{w}_k, \quad \forall k \quad (79)$$

$$f(l_{k4}, \bar{l}_{k4}) \geq p_k, \quad \forall k \quad (80)$$

$$f(n_{kj}, \bar{n}_{kj}) \geq \begin{cases} \mathbf{w}_j^H (\mathbf{h}_{k1} \mathbf{h}_{k1}^H + \mathbf{h}_{k2} \mathbf{h}_{k2}^H) \mathbf{w}_j, & \forall j < k \\ |\mathbf{h}_{k2}^H \mathbf{w}_j|^2, & \forall j > k \end{cases}, \quad \forall k \quad (81)$$

$$(\mathbf{H}_1^{<k})^H \mathbf{w}_k = \mathbf{0}, \quad \forall k \quad (82)$$

$$\|\mathbf{w}_k\| \leq 1, \quad \forall k \quad (83)$$

$$\sum_k (p_{k1} + p_{k2}) \leq P. \quad (84)$$

- [6] J. So and Y. Sung, "Improving non-orthogonal multiple access by forming relaying broadcast channels," *IEEE Communications Letters*, vol. 20, pp. 1816-1819, Sep. 2016.
- [7] B. Kim, S. Lim, H. Kim, S. Suh, J. Kwun, S. Choi, C. Lee, S. Lee, and D. Hong, "Non-orthogonal multiple access in a downlink multiuser beamforming system," in *Proc. MILCOM*, pp. 1278-1283, 2013.
- [8] Y. Lan, A. Benjebboiu, X. Chen, A. Li, and H. Jiang, "Considerations on downlink non-orthogonal multiple access (NOMA) combined with closed-loop SU-MIMO," in *IEEE ICSPCS, 2014 8th International Conference on*, pp. 1-5, 2014.
- [9] S. Liu, C. Zhang, and G. Lyu., "User selection and power schedule for downlink non-orthogonal multiple access (NOMA) system," in *Proc. IEEE ICCW*, pp. 2561-2565, 2015.
- [10] M. F. Hanif, Z. Ding, T. Ratnarajah, and G. K. Karagiannidis, "A minorization-maximization method for optimizing sum rate in the downlink of non-orthogonal multiple access systems," *IEEE Trans. Signal Process.*, vol. 64, pp. 76-88, Jan. 2016.
- [11] Z. Ding, F. Adachi, and H. V. Poor., "The application of MIMO to nonorthogonal multiple access," *IEEE Trans. Wireless Commun.*, vol. 15, pp. 537-552, Jan. 2016.
- [12] A. Sayed-Ahmed and M. Elsbrouty, "User selection and power allocation for guaranteed SIC detection in downlink beamforming nonorthogonal multiple access," in *Proc. IEEE Wireless Days*, pp. 188-193, 2017.
- [13] J. Seo and Y. Sung, "Beam design and user scheduling for nonorthogonal multiple access with multiple antennas based on Pareto optimality," *IEEE Trans. Signal Process.*, vol. 66, pp. 2876-2891, Jun. 2018.
- [14] Z. Chen, Z. Ding, and X. Dai, "Beamforming for combating inter-cluster and intra-cluster interference in hybrid NOMA systems," *IEEE Access*, vol. 4, pp. 4452-4463, Aug. 2016.
- [15] Z. Chen, Z. Ding, X. Dai, and G. K. Karagiannidis, "On the application of quasi-degradation to MISO-NOMA downlink," *IEEE Trans. Signal Process.*, vol. 64, pp. 6174-6189, Aug. 2016.
- [16] T. Yoo and A. Goldsmith, "On the optimality of multiantenna broadcast scheduling using zero-forcing beamforming," *IEEE J. Sel. Areas in Commun.*, vol. 24, pp. 528-541, Mar. 2006.
- [17] J. Choi, "Minimum power multicast beamforming with superposition coding for multiresolution broadcast and application to NOMA systems," *IEEE Trans. Commun.*, vol. 63, pp. 791-800, Mar. 2015.
- [18] H. Harashima and H. Miyakawa, "Matched-transmission technique for channels with intersymbol interference," *IEEE Trans. Commun.*, vol. 20, pp. 774-780, Aug. 1972.
- [19] M. Tomlinson, "New automatic equaliser employing modulo arithmetic," *Electron. Lett.*, vol. 7, pp. 138-139, Mar. 1971.
- [20] C. Windpassinger, R. F. H. Fischer, T. Vencel, and J. B. Huber, "Precoding in multiantenna and multiuser communications," *IEEE Trans. Wireless Commun.*, vol. 3, pp. 1305-1316, Jul. 2004.
- [21] D. Tse and P. Viswanath, *Fundamentals of Wireless Communications*. Cambridge, U.K.: Cambridge University Press, 2005.
- [22] G. Scutari, F. Facchinei, and L. Lampariello, "Parallel and distributed methods for constrained nonconvex optimization - Part I: Theory," *IEEE Trans. Signal Process.*, vol. 65, pp. 1929-1944, Apr. 2017.
- [23] W.-C. Li, T.-H. Chang, C. Lin, and C.-Y. Chi, "Coordinated beamforming for multiuser MISO interference channel under rate outage constraints," *IEEE Trans. Signal Process.*, vol. 61, pp. 1087-1103, Mar. 2013.